Available online at www.sciencedirect.com
SCIENCE DIRECT®
Journal of Nuclear Materials 327 (2004) 194–201
journal of nuclear materials
www.elsevier.com/locate/jnucmat

Corrosion of nickel in molten LiCl–Li_2O at 750 °C

R.Y. Liu *, X. Wang, J.S. Zhang, X.M. Wang

Department of Materials Engineering, Dalian University of Technology, Dalian 116024, PR China

Received 18 August 2003; accepted 12 February 2004

Abstract

Corrosion of the reduction vessel induced by molten LiCl–Li_2O is an important problem in the lithium reduction technique for the spent nuclear fuel management. This study investigates the corrosion of nickel in molten LiCl–10 wt% Li_2O at 750 °C by immersion experiments, with the aim of unraveling the corrosion behavior. Nickel corrodes very fast in the melt, forming a layer of NiO, which is converted to $Li_2Ni_8O_{10}$ and then to $LiNiO_2$. The weight loss curve shows a linear rate law, which is owing to the harmful reaction between oxides and melt at the melt/scale boundary with the formation of the porous corrosion scale. The corrosion mechanism of nickel is also discussed.

PACS: 82.45.Bb

1. Introduction

A lithium reduction technique has been developed for the spent nuclear fuel management [1]. In the process the oxide (UO_2) is reduced to the metallic form (U) by reaction with lithium dissolved in molten LiCl at 750 °C. The technique can effectively reduce the volume and radiation of the spent nuclear fuel, which benefits to the disposal of the spent nuclear fuel. The strong basic oxide Li_2O formed during the reduction process is dissolved in the molten salt. In the reduction condition, the environment is mainly lithium chloride with dissolved Li_2O (about 10 wt%) under air or O_2–Ar. Thus the containment materials used in the technique undertake severe corrosion attack induced by the Li_2O in molten LiCl–Li_2O mixture. Corrosion in the fuel reduction condition, i.e., harmful reactions between the containment materials and the molten salt, resulted in delay of the application of the new technique.

To date, only several reports have been published on the corrosion of materials in molten LiCl–Li_2O, with the main objective to find a material that can be used to improve the vessel longevity for this new technology [1–3]. In those studies, many iron-base and nickel-base alloys with high temperature oxidation resistance have been investigated in molten LiCl–Li_2O. Unfortunately, those alloys all experience the serious corrosion in such molten salts. In other words, these alloys cannot offer the adequate longevity as the container materials for the new technology.

The mechanism and the rate of the corrosion of a metal in molten LiCl–Li_2O is thus not clear. In the present work the corrosion of nickel has been studied in molten LiCl–Li_2O at 750 °C under air with immersion test. Nickel was chosen because it is the main element in nickel-base alloys and an important element in iron-base alloys. To our knowledge it is the first time that nickel has been studied in molten LiCl–Li_2O with the aim of unraveling the corrosion behavior.

2. Experimental procedure

Pure nickel (99.9%) plate was used for the metallic specimens. Rectangular specimens of a size, 15 mm × 10 mm × 4 mm, were cut from the plate. They were polished with No. 1000SiC paper on all sides, ultrasonically

* Corresponding author. Tel.: +86-411 470 8469; fax: +86-411 470 9284.
E-mail address: jszhang@dlut.edu.cn (R.Y. Liu).

0022-3115/$ - see front matter © 2004 Elsevier B.V. All rights reserved.
doi:10.1016/j.jnucmat.2004.02.006

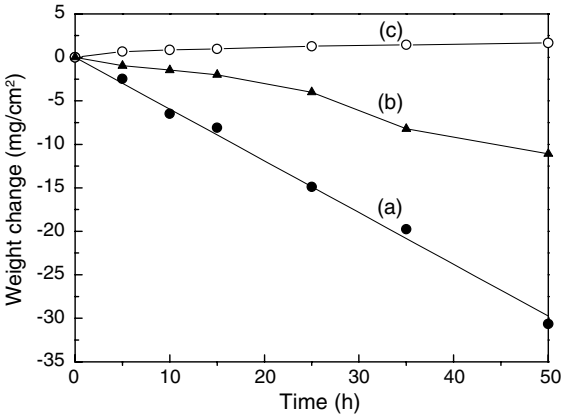

Fig. 1. Corrosion kinetic curves for nickel with and without molten LiCl–Li_2O at 750 °C under air, as function of time; (a) weight loss in molten LiCl–Li_2O with stripping the products, (b) weight loss in molten LiCl–Li_2O without stripping the products, (c) weight gain without molten LiCl–Li_2O.

cleaned in acetone, rinsed with distilled water, dehydrated by ethanol and dried.

High purity reagent of LiCl and Li_2O were used. Impurity contents in wt% are Na < 0.2%, Ca < 0.05%, Fe < 0.001%, SO_4 < 0.05% and H_2O < 0.43% for LiCl and Ca < 0.01%, Fe < 0.01%, and Si < 0.01 % for Li_2O. Immersion experiments were carried out at 750 °C in a LiCl–10 wt% Li_2O melt under air, with the aim of simulating the fuel reduction condition. For every group of experiments, the 22 g salt contained in an alumina crucible of 25 ml was used. The distance from the molten salt/atmosphere interface to the specimen surface was about 10 mm. The salts contained in an alumina crucible were dried at 350 °C for 24 h and then melted at 750 °C. The specimens were measured in weights and sizes before immersion in molten salts. After selected period of time, the specimens were taken out of the melt, rinsed with distilled water, dipped in a solution containing hydrochloric acid and tetrabutylammonium iodide to strip corrosion products, dried, and weighed by a

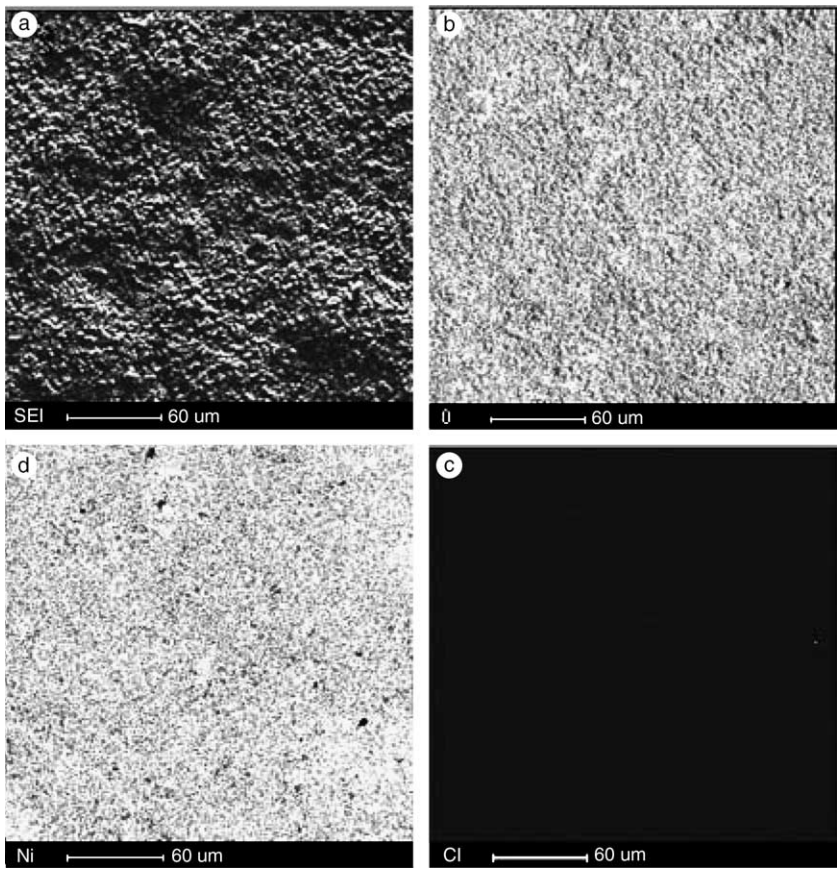

Fig. 2. Corrosion layer morphology and elements distribution for nickel in molten LiCl–Li_2O at 750 °C for 5 h; (a) SEI, (b) O distribution, (c) Ni distribution, (d) Cl distribution.

microbalance. Additionally, the corroded specimens without stripping corrosion product were also weighed by the microbalance for the purpose of evaluating the possible dissolution of oxide in the melt. To evaluate the effect of the salt on the corrosion of the materials, the oxidation of nickel without the salt under air at 750 °C was also conducted by discontinuously measuring their weight change.

The corroded specimens were analyzed by X-ray diffraction (XRD), electron probe microanalysis (EPMA) and scanning electron microscopy (SEM) coupled with energy dispersive X-ray microanalysis (EDX).

3. Results

3.1. Corrosion kinetics

The weight-change curves for the corrosion of nickel with and without the melt at 750 °C under air are shown in Fig. 1. The presence of the molten salt significantly accelerates the corrosion of nickel. The weight gain curve of nickel without melt shows a parabolic one (Fig. 3(c)). However the weight loss of nickel increased linearly in molten LiCl–Li_2O (Fig. 1(a)), implying that non-protective corrosion scale formed during immersion test. The weight loss of nickel in molten LiCl–Li_2O without stripping the corrosion products is given in Fig. 1(b), with the aim of testing the possibility of dissolution of nickel oxide in the melt. The experimental data in Fig. 1(b) were higher than exact data because spallation was observed for the corroded specimens after immersion for 25 h, and especially for 35 and 50 h. However it seems logical to deduce that dissolution of nickel oxide should take place in the melt during the immersion test.

3.2. Corrosion products

During the experiments, nearly no spallation of the corrosion scales was observed before 15 h, the obvious spallation of the scales appeared after 25 h. Severe spallation was observed on the surface of the specimens

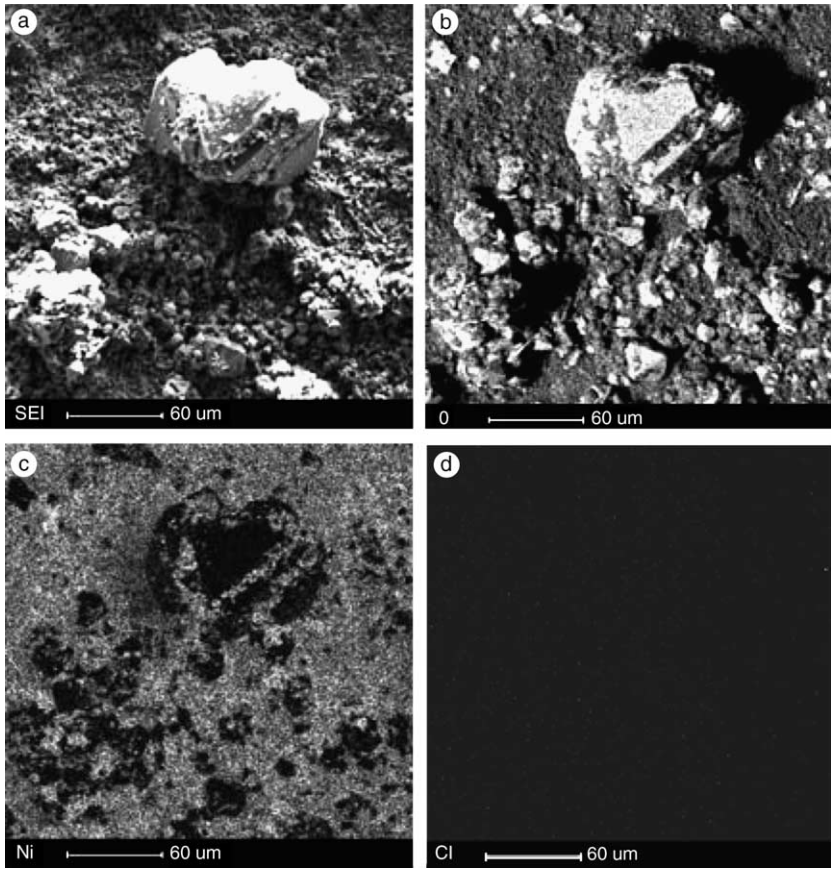

Fig. 3. Corrosion layer morphology and elements distribution for nickel in molten LiCl–Li_2O at 750 °C for 50 h; (a) SEI, (b) O distribution, (c) Ni distribution, (d) Cl distribution.

corroded for 35 and 50 h. The electron probe micrograph and elements distribution of surface of the corroded specimen in molten LiCl–Li_2O for 5 h was shown in Fig. 2. The product formed on the surface, is seriously poor in chlorine, and the distribution of both nickel and oxygen keeps well-proportioned, which implies compact corrosion scale formed on the surface without formation of any chlorides. Fig. 3 gives the electron probe micrograph and element distribution of the surface of the corroded specimen after immersion for 50 h. Accidental morphology was observed on the surface of the specimen in Fig. 3(a). The protuberant areas (white) are rich in oxygen, and the concave areas (dark) are rich in nickel and poor in oxygen. In combination with the severe spallation of the specimen, it is reasonable to believe that the concave areas are the exposed matrix nickel being ascribed to the spallation of corrosion scale formed here and that the protuberant areas are the remained oxides. And therefore it can be deduced that the corrosion scale was not compact and stable after immersion for 50 h. Additionally, no chloride was detected on the surface as shown in Fig. 3(d).

Fig. 4 gives the XRD analysis of corrosion products of nickel in molten LiCl–Li_2O at 750 °C after various immersion periods of time. Only NiO was detected on the surface of nickel after 5 h, and the oxide layers on nickel corroded for 15 h were composed of NiO and $Li_2Ni_8O_{10}$. NiO, $Li_2Ni_8O_{10}$ and $LiNiO_2$ were detected on the surface of nickel corroded for 25 and 50 h. According to the standard XRD patterns, the three diffraction angles (2Theta) of $Li_2Ni_8O_{10}$ with the strongest peak values are 37.865°, 43.998° and 63.998°. In Fig. 4(d) and (e), the peak of $Li_2Ni_8O_{10}$ at 63.998° which appeared in Fig. 4(c) was not detected, and the other peaks overlapped with those of NiO or $LiNiO_2$. Thus it can be deduced that the corrosion products of nickel corroded for 25 or 50 h were mainly composed of NiO and $LiNiO_2$ and corrosion layer contained no or a small degree of $Li_2Ni_8O_{10}$.

The cross-sectional morphologies of nickel corroded for various periods of time in molten LiCl–Li_2O under air at 750 °C are shown in Fig. 5. A compact scale of about 5 μm thick was formed on the surface of specimen corroded for 5 h (Fig. 5(a)). Some porosity can be observed on the scale (Fig. 5(a)), which may be related to the outward diffusion of nickel. EDX and XRD analysis (Fig. 4(b)) indicates that the products on the specimen consist only of NiO and contain no chlorides and Li-containing oxides. As shown in Fig. 5(b), the two-layered scale formed on the specimen corroded for 15 h was still compact. The EDX analysis shows that the ratio of atomic percentage of nickel/oxygen in outer layer is 43.54:56.46 (close to 8:10) and that in inner layer is 48.37:51.63 (close to 1:1) (lithium cannot be detected by EDX). Combining with both the result of EDX and the XRD analysis (Fig. 4(c)), the outer scale should be rich in $Li_2Ni_8O_{10}$ and the inner scale should be rich in NiO. Porous scale was observed on the surface of specimens corroded for 25 and 50 h, and no obvious phase boundary could be detected on the scale. Since the

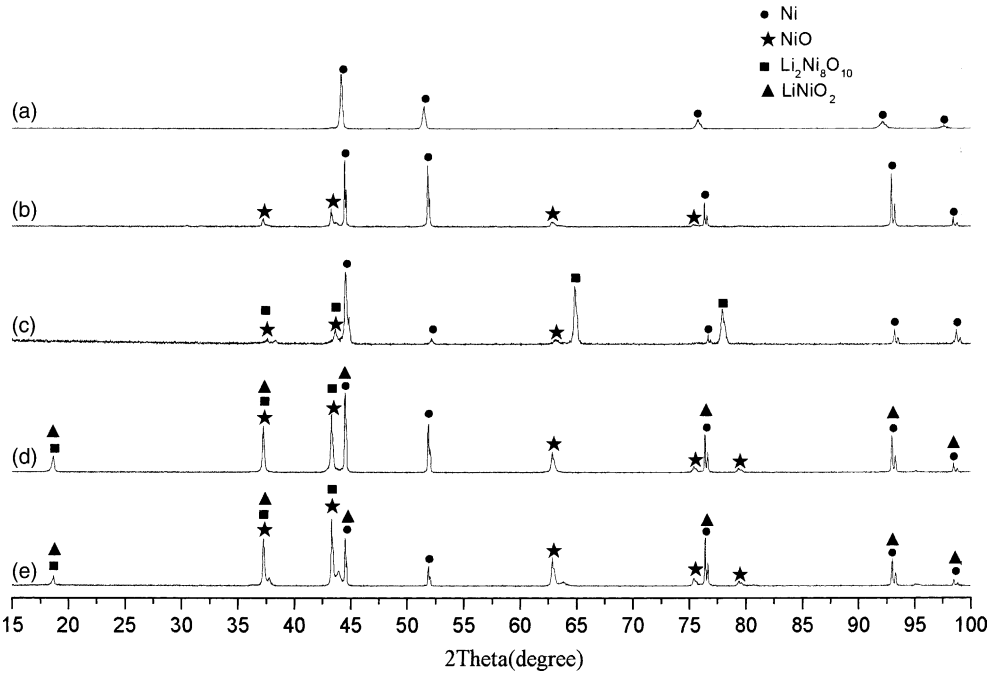

Fig. 4. XRD pattern of nickel in molten LiCl–L_2O at 750 °C after various immersion times; (a) 0 h, (b) 5 h, (c) 15 h, (d) 25 h, (e) 50 h.

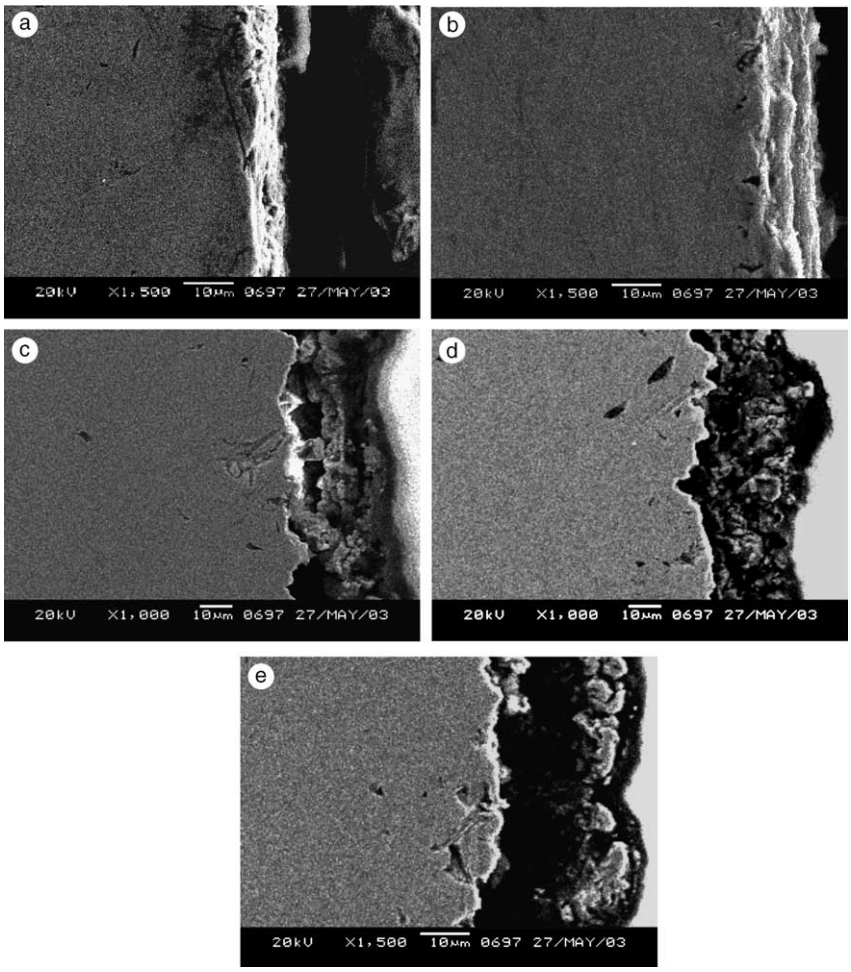

Fig. 5. Cross-sectional morphologies of nickel corroded at 750 °C for various periods of time; (a) 5 h, (b) 15 h, (C) 25 h, (d) 50 h, (e) 50 h.

corrosion scale was not compact, the EDX analysis data cannot reflect the exact element component of the scale. Therefore, the XRD analysis should be the exclusive method to identify the corrosion products. As shown in Fig. 4(d) and (e), the porous scale is mainly composed of NiO and $LiNiO_2$. Moreover obvious crack was observed at some areas in the corrosion scale as shown in Fig. 5(e). The EPMA analysis can clearly show that the corrosion scale only partially adhered to the base metal and contained no chlorides, as shown in Fig. 6. Considering the results of SEM and EPMA, it can be concluded that the corrosion scale was non-protective during long time immersion test.

4. Discussion

The experimental results indicated that no chlorides were detected in the corrosion products and corrosion characteristic is far from that of 'active oxidation' induced by hot corrosion of molten chlorides salts coatings or of chlorine [4–6]. Thus it can be deduced that the active oxidation mechanism becomes impossible in this experiment. Moreover the chloride ion has little effect on the basic dissolution of oxides, which proved by the study of Deanhardt and Stern [7]. So the effect of chloride ion on the corrosion in the melt can be neglected.

Corrosion in molten salts is characterized by two steps. The first is oxidation of the metal and the second is basic or acidic dissolution of the oxide scale [8]. For oxidation, oxygen has to diffuse through the melt to metal surface. It may be provided either by dissolution from the gas phase or by dissociation of oxygen bearing molecules in the molten salts. In this work the concentration of strong basic Li_2O in the melt is 10 wt%, which may result in basic dissolution in the corrosion process. During immersion in molten LiCl–Li_2O, initially, NiO was formed by reaction with oxygen dissolved from the

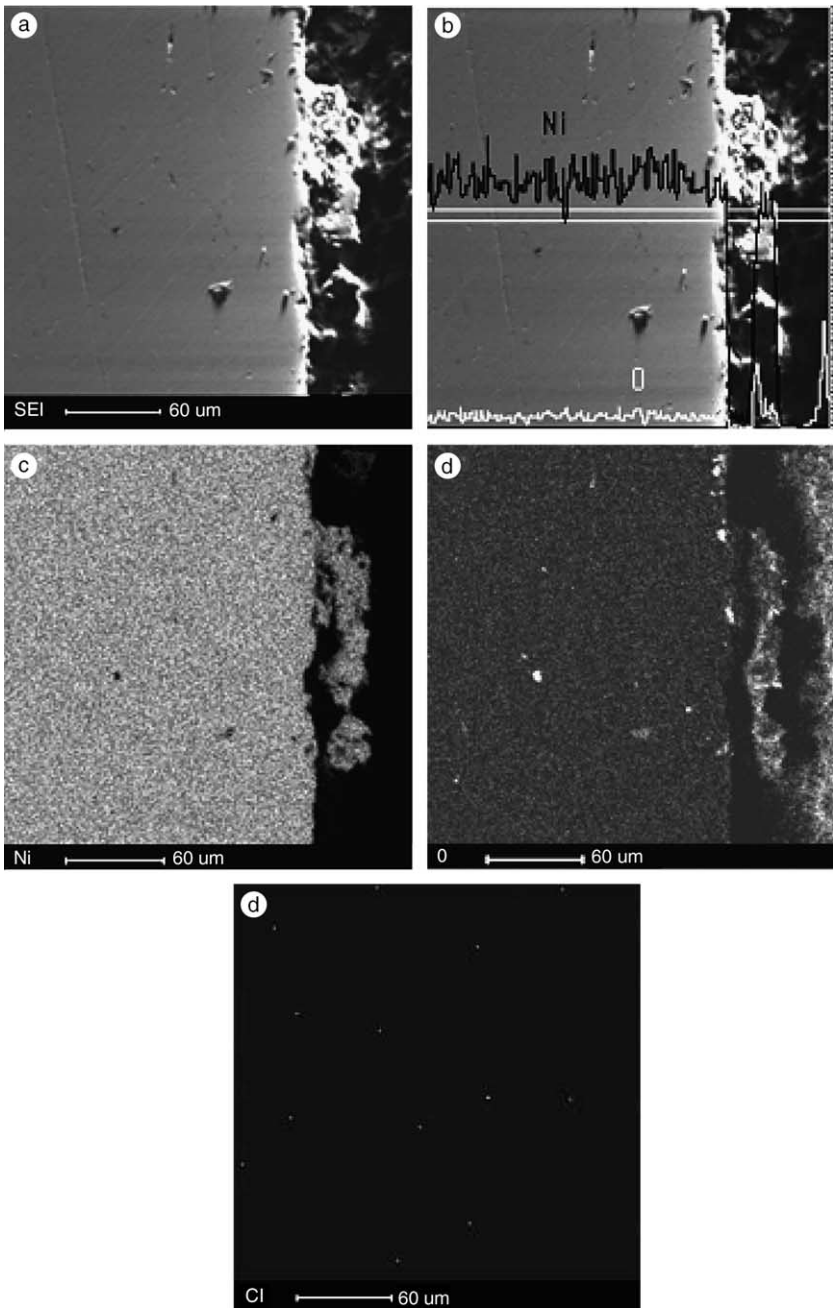

Fig. 6. Secondary electron image and elements distribution in a cross-section of nickel in molten LiCl–Li_2O at 750 °C for 50 h (a) SEI, (b) line analysis, (c) Ni distribution, (d) O distribution, (e) Cl distribution.

air in the melt, and might be accompanied by succeeding dissolution of NiO [9]

$$NiO + O^{2-} = NiO_2^{2-} \quad (1)$$

which is equivalent to

$$NiO + Li_2O = Li_2NiO_2. \quad (1a)$$

The O^{2-} ions (Li_2O) consumed by reaction (1) at the interface of oxide/melt would be delivered continuously by the melt. Therefore the concentration of O^{2-} ions will be low at the interface of oxide/melt and high at the interface of melt/gas. In other words, the gradient of concentration of O^{2-} ions from the interface of oxide/melt to the interface of melt/gas is positive. In this case,

no precipitation of NiO takes place, since no negative solubility gradient will be established in the melt. Thus the traditional fluxing-precipitation mechanism [10] can be neglected in this experiment. So the weight loss of nickel without stripping (as shown in Fig. 1(b)) should be owing to the dissolution of NiO through reaction (1).

On the other hand, stable layers of corrosion products of $Li_2Ni_8O_{10}$ and $LiNiO_2$ were formed in the melt. From the experimental results the following reaction sequence for the insoluble corrosion products is suggested:

(1) Formation of NiO (5 h).
(2) Lithiation reaction of NiO with forming $Li_2Ni_8O_{10}$ (15 h).
(3) Transformation reaction form $Li_2Ni_8O_{10}$ to $LiNiO_2$ (25 h).

Fig. 7 describes the processes of corrosion of nickel in the molten LiCl–Li_2O.

With the development of corrosion, further oxidation of NiO occurs through the lithiation process in the melt. The lithiation reactions of NiO with Li_2O and oxygen take place at the interface of the corrosion-scale/melt. Generally, the lithiation reaction of NiO can be described as [11]

$$2Li_2O + 4NiO + O_2 = 4LiNiO_2. \quad (2)$$

Due to less solubility of oxygen in melts under air atmosphere, the incomplete lithiation process of NiO leads to products of producing $Li_2Ni_8O_{10}$ [11] after corrosion for 15 h ($Li_2Ni_8O_{10}$ can be regarded as 2Li-NiO_2+6NiO [12]). The forming reaction of $Li_2Ni_8O_{10}$ at the interface of melt/scale should be

$$2Li_2O + 16NiO + O_2 = 2Li_2Ni_8O_{10}. \quad (3)$$

Considering the compact outer layer of $Li_2Ni_8O_{10}$ in Fig. 5(b), the growth of $Li_2Ni_8O_{10}$ should take into account the outward diffusion of nickel through the whole scale to the scale/melt phase boundary. It seems likely to assume that the compact scale formed after immersion for 15 h could retard further corrosion attack. However the fact is that the porous scale (composed of $LiNiO_2$ and NiO) replaced the compact scale with the ongoing corrosion, as shown in Fig. 5(c) and (d). This may be ascribed to the instability of $L_2Ni_8O_{10}$ in molten LiCl–Li_2O, which results in the transformation reaction from $Li_2Ni_8O_{10}$ to $LiNiO_2$ in contact with melt. The transformation reaction can be represented by

$$2Li_2Ni_8O_{10} + 6Li_2O + 3O_2 = 16LiNiO_2. \quad (4)$$

The XRD analysis indicated that $LiNiO_2$ is the only stationary Li-containing oxide in molten LiCl–Li_2O during long time immersion. Unfortunately, with the formation of $LiNiO_2$, spallation of the scale took place over a considerable surface area and the porous scale formed on the surface. Therefore it seems reasonable to believe that $LiNiO_2$ has poor adhesion with both base metal and other oxides (NiO or $Li_2Ni_8O_{10}$) and is easily to peel off in the melt. Thus it can be concluded that the formation of $LiNiO_2$ destroyed the integrity of corrosion scale after corroded for long time (>25 h). The porous corrosion scale cannot provide an effective barrier to the

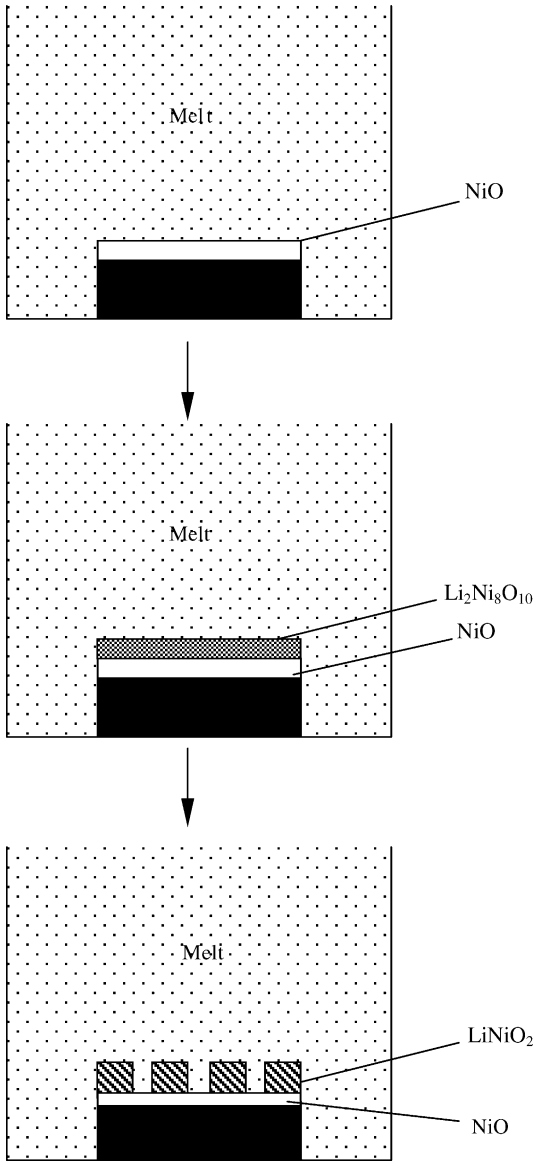

Fig. 7. Schematic diagrams of the corrosion processes of nickel in the molten LiCl–Li_2O during the total experimental time.

diffusion of oxygen and melt, resulting in the severe corrosion attack of nickel in the melt.

The linear weight loss curve could be explained by Wagner's theory [13,14]. Based on the Wagner's theory, when the corrosion curve follows linear rate law, the corrosion process is determined by the reaction at the interface of oxide/media and the corrosion rate is to be independent of thickness of corrosion scale. Thus it can be concluded that the linear weight loss curve comes mainly from the contribution of the harmful reaction between the oxides and melt at the interface melt/scale accompanied by the formation of non-protective scale.

5. Conclusions

The presence of the melt accelerates significantly the corrosion of nickel. Nickel shows very fast corrosion in the melt with formation of layer of NiO (5 h) after short corrosion time (5 h), of NiO and $Li_2Ni_8O_{10}$ after corroded for 15 h, and of NiO and $LiNiO_2$ after longer periods of time (25–50 h). The weight loss curve shows a linear rate law, which is mainly related to harmful reaction between the oxides and melts at the interface of melt/scale accompanied by the formation of non-protective scale.

Acknowledgements

The authors wish to express their thanks to Professors D.H. Wang and M.K. Lei for technical assistance and helpful discussion.

References

[1] J.E. Indacpchea, J.L. Smith, J. Mater. Res. 14 (5) (1999) 1990.
[2] S.H. Cho, J.S. Zhang, P.K. Shins, Korean J. Mater. Res. 9 (2) (1999) 211.
[3] S.H. Cho, S.C. Park, J.S. Zhang, Korean J. Mater. Res. 9 (9) (1999) 985.
[4] E. Reese, H.J. Grabke, Mater. Corros. 43 (1993) 547.
[5] E. Reese, H.J. Grabke, Mater. Corros. 44 (1994) 41.
[6] Y.Y. Lee, M.J. Mcnallan, Metall. Trans. A 18A (1987) 1099.
[7] M.L. Deanhardt, K.H. Stern, J. Electrochem. Soc. 128 (1981) 2577.
[8] M. Spiegel, P. Biedenkopf, Grabke, Corros. Sci. 39 (1997) 1193.
[9] J.A. Goebel, F.S. Pettit, Metall. Trans. A 1 (1970) 1943.
[10] R.A. Rapp, Corros. Sci. 44 (2002) 209.
[11] S. Xu, Y. Zhou, X. Huang, J. Power Sources 103 (2002) 230.
[12] H. Xing, X. Songbo, Z.E. Bangna, J. Shanghai Univ. 6 (2000) 1999.
[13] M.A. Espinosa, G. Carbaja, Mater. Corros. 54 (2003) 304.
[14] P. Kofstad, High temperature corrosion, Elsevier Applied Science, London, 1988.